Structure Development in High-Speed Spinning of Polyethylene Naphthalate (PEN) Fibers

M. CAKMAK, J. C. KIM

Polymer Engineering Institute, University of Akron, Akron, Ohio 44325–0301

Received 17 November 1995; accepted 9 August 1996

ABSTRACT: The structural evolution in fibers produced by high-speed fiber spinning of Polyethylene 2,6 naphthalene dicarboxylate (polyethylene naphthalate) was investigated. The fibers were found to remain amorphous at speeds up to 2500 m/min, and subsequent increases in speed resulted in highly oriented crystalline domains containing primarily α crystalline modification. The fibers processed at and above 3500 m/min were found to contain the β modification together with the α modification. At the highest speed investigated, 4000 m/min, the crystalline regions became disordered, and this was attributed to low deformation temperatures that accompany neck-like deformation. Constrained annealing of the fibers results in relatively unoriented crystalline structure at 500 m/min. Although the WAXS patterns of fibers spun in the 1000–2500 m/min range do not show any crystalline peaks, these fibers develop crystalline regions with significant orientation upon constrained annealing. In addition, these regions were found to have both α and β crystalline phases, indicating that not only the α but also the β phase can be grown from the oriented amorphous precursors upon constrained annealing. From our experimental results we extrapolated a value of 0.791 100% crystalline PEN. The estimated intrinsic birefringence value for the amorphous PEN is 0.75. © 1997 John Wiley & Sons, Inc. J Appl Polym Sci **64:** 729–747, 1997

INTRODUCTION

The increased use of higher take-up speeds (4000–6000 m/min) in commercial operations necessitates the research on fundamental understanding of the influence of such high spinning speeds on the structure development and resulting properties. This then enables the engineers to determine the processing window in which to operate in order to obtain fibers with desired properties.

Polyethylene 2,6-naphthalene dicarboxylate, PEN, being a slow-crystallizing polymer, resembles in its rheological, thermal, and crystallographic behaviors, to its well-studied homologue polyethylene terephthalate.[1–5] In some respects PEN exhibits its own unique characteristics, such as a higher melt viscosity than PET, and it is polymorphic, exhibiting two crystal structures (called α[6] and β[7]). The α-modification has a triclinic unit cell with the following cell parameters; a = 0.651 nm b = 0.575 nm c = 1.32 nm α = 81.33° β = 144°, and γ = 100°, and density of 1.407 g/cm^3. Another crystalline form, called the β-modification, was observed and partially characterized by Buchner and Zachmann in 1989. It is also triclinic with a = 0.926 nm, b = 1.559 nm, c = 1.273 nm, α = 121.6°, β = 95.57°, and γ = 122.52°. The density is calculated as 1.439 g/cm^3. The chains are not completely extended and every naphthalene ring is twisted about the chain axis by 180°. The density of 100% amorphous PEN is reported

Correspondence to: M. Cakmak.

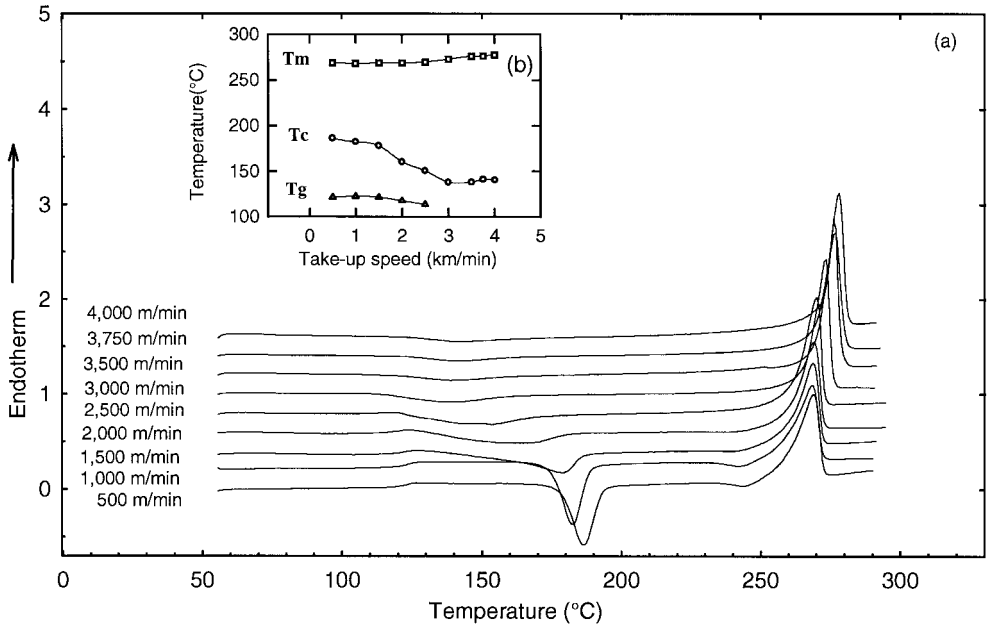

Figure 1 DSC spectra on PEN fibers spun at different take-up speeds.

to be 1.34 g/cm^3 by Buchner et al.[7] and 1.325 g/cm^3 by Ouchi et al.[8]

Thermal properties of PEN were studied in detail.[9] The equilibrium melting parameters were estimated to be T_m = 610 K, heat of fusion, ΔH_f = 25 ± 2 KJ/mol, and ΔS_f = 41 ± 3.3 J/Kmol. The glass transition temperature was T_g = 382.3 ± 2.03 × ln q (q in K/min).

The effect of uni- and biaxial deformation on structure development in PEN films were studied by Hayashi et al.[10] as well as by our group and collaborators.[11,12] These studies indicate that upon stretching, the naphthalene planes readily orient parallel to the broad surface of the films even in the uniaxial free width stretching mode. Our studies[11] also indicate that simultaneous biaxial stretching results in bimodal orientation of the chain axes along the two machine directions. PEN[13] was found to exhibit a distinct neck during deformation at temperatures between the glass transition temperature and cold crystallization temperature. This was attributed to highly localized rapid alignment of naphthalene planes parallel to the broad surfaces if the samples manifesting itself macroscopically as a neck. In a later study , we were able to eliminate this neck formation by blending PEN with PEI.[14] The PEN/PEI blends are miscible and with addition of small amount of PEI helped eliminated this neck formation by increasing the interchain friction between the PEN molecules as evidenced by the increase in drawing stress in the stress–strain curves. In addition, the PEI chains were found to disrupt the naphthalene plane orientation parallel to the surfaces of the films. Injection-molded PEN parts were found to exhibit three layer amorphous skin-shear crystallized subskin and amorphous core structure at low mold temperatures and injection speeds.[15] The shear-induced crystallized sublayers were also found to exhibit this preferential orientation of naphthalene planes parallel to the broad surfaces of the parts. These regions were found to have a plate-like texture, and this structure was found to delaminate quite readily under tensile or shear deformations at low temperatures.

In this article we will present our results on the development of structure in fibers as influenced by the take-up speed and subsequent heat setting stage.

Materials and Experimental Procedures

The polyethylene 2,6-naphthalene dicarboxylate, PEN of 0.825 dL/g IV, was provided by Goodyear Polyester Division (now Shell Polyester). The pellets were dried overnight in a vacuum oven set at 150°C. The fibers were produced using an extruder of 30 mm diameter attached to a metering pump. The temperature profile of 220, 285, and

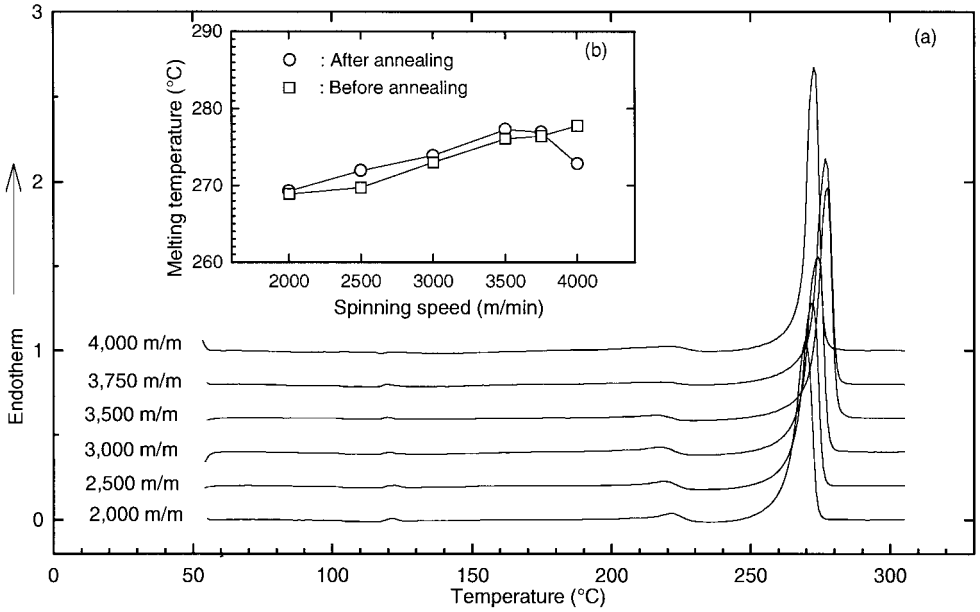

Figure 2 DSC thermograms of annealed PEN fibers. Fibers were annealed at 220°C for 20 min. Numbers indicate the take-up speed. (b) Melting temperatures.

300°C was used along the extruder. The die, attached to the exit of the metering pump, had 3 × 1 mm crossectional dimensions. A high-speed winder was used to make fibers at different speeds. The spinline length between the die and the take-up winder was approximately 2 meters. For a separate set of experiments, the fibers were wound on a square sandwich frame and annealed at 220°C for 20 min. The frame prevented the shrinkage.

The thermal behavior of the fibers was analyzed using a Perkin–Elmer DSC 7, which scanned the samples at a heating rate of 10°C/min in a dry nitrogen atmosphere. The fiber birefringences were obtained using a Leitz Labolux Polarizing microscope with a 30 order Berec compensator. In order to ascertain the phase behavior and crystallinity in these fibers, a series of WAXS film patterns as well as equatorial diffractometer scans were obtained on as-spun as well as annealed fibers. The room temperature tensile behavior of the fibers was obtained using a Instron tensile tester (Model 4204) with a gauge length of 2.5 cm. using a 100%/min testing rate. For each condition, five samples were tested and the results were averaged. The fracture surfaces of the tensile tested fibers were examined using an ISI SX40 scanning electron microscope.

RESULTS

Thermal Behavior

When the spinline speed is increased, the DSC spectra shows significant changes, as indicated in Figure 1. At low take-up speeds, the area under the cold crystallization peak located around 188°C is about the same as that of the melting peak situated in 245–170°C range, indicating that these fibers contained very little crystallinities before this DSC scan took place. As the spinning speed is increased, the cold crystallization peak moves to lower temperatures [see Fig. 1(b) in the inset] and begins to broaden. This is a typical behavior of polyester type polymers with a low crystallization character and directly relates to the reduction of entropy with preferential orientation during the melt spinning. As the temperature is increased past the glass transition, those chains that did not crystallize during spinning, but had attained significant levels of orientation, crystallize. The chains that orient to a larger extent during the melt spinning actually require lower thermal energy to crystallize, and this occurs at lower temperature. In this sense, the breadth of the cold crystallization peak may reflect the orientation distribution in the uncrystallized regions of these

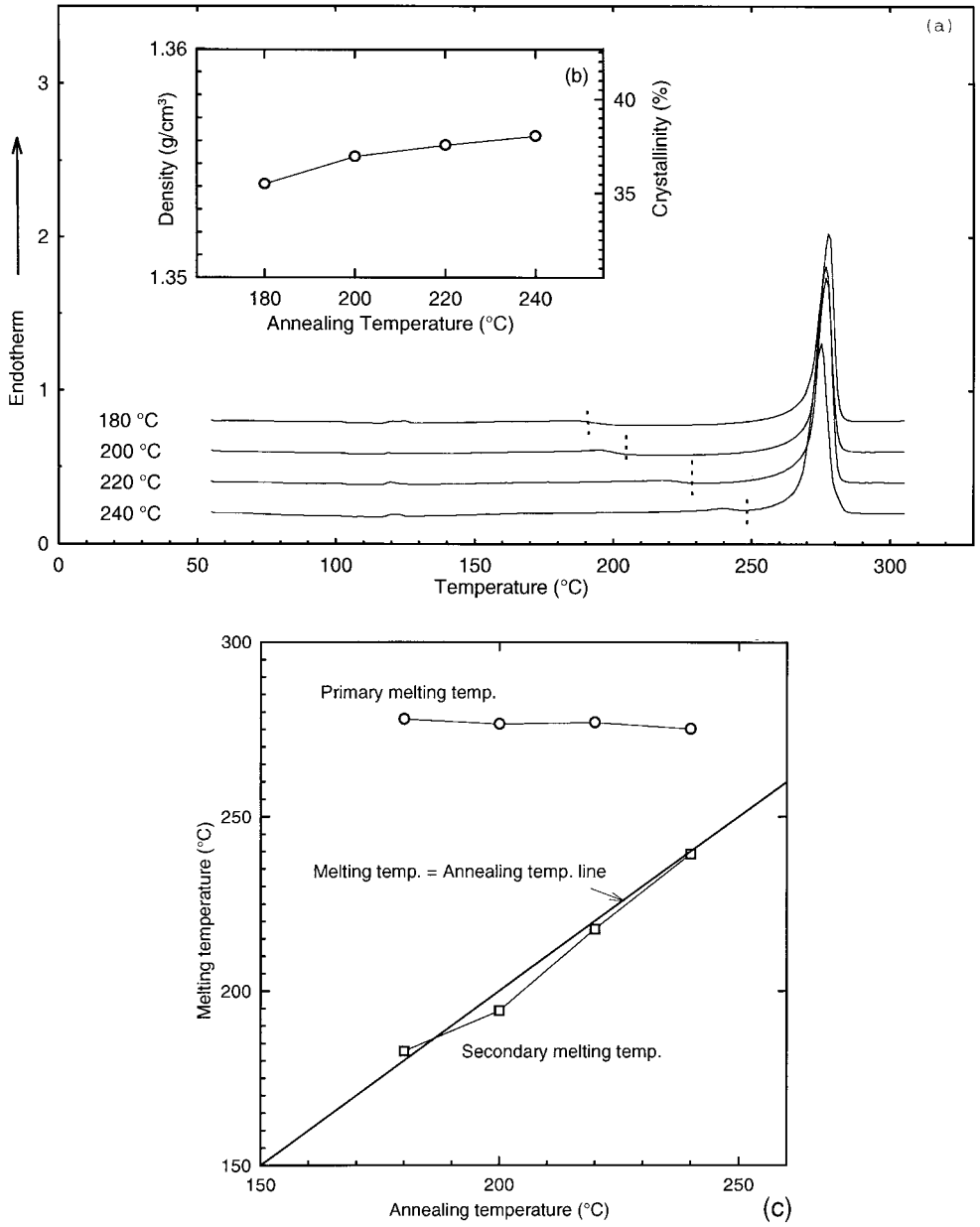

Figure 3 DSC curves of PEN fibers spun at 3750 m/min and annealed at different temperatures for 20 min. (c) Melting temperatures of PEN fibers that were annealed at different temperatures for 20 min. Fibers were spun at 3750 m/min.

highly oriented fibers prior to the DSC scan. As an increasing fraction of polymer chains are crystallized with increased spinning speed, the amount of material that crystallizes during the subsequent DSC scan decreases. This, in turn, explains the reduction and eventual disappearance of the cold crystallization peak at higher spinning speeds.

In these DSC spectra, we also observe that the melting peak position remains constant between 500 m/min to 2000 m/min. Beyond this speed, it begins to increase from 268.9°C at 2000 m/min to 277.8°C at a take-up speed of 4000 m/min. This increase may be attributed to the increase of crystallite size, the increase of crystal perfection, and possibly a phase change. In order to ascertain which one of these factors, or their combinations, are in effect here, we need to examine the men-

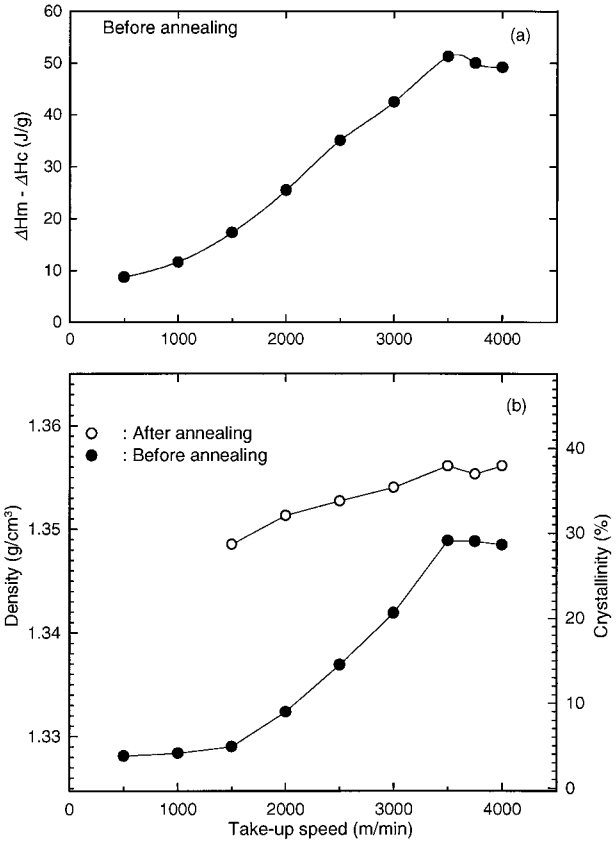

Figure 4 Crystallinity of PEN fibers vs. take-up speed.

tioned structural features using x-ray techniques. This will be discussed in the following sections.

When these fibers were annealed at 220°C for 20 min with their lengths constrained, the cold crystallization peak disappears from the DSC spectra as a result of increased crystallinity (Fig. 2). We do, however, still see the increase of melting peak with the increase of take-up speed and, in addition, we observe a slight decrease of T_m between 3750 to 4000 m/min. This appears to be related to the crystal structure, which we shall discuss later. As is typical of these types of polymers, when annealed, the PEN fibers also exhibit a small endotherm in their DSCs situated about 5–10°C above the annealing temperature. This secondary melting at the crystallization temperature is a well-known phenomenon in several polycondensation polymers such as PET, PBT, PEEK, PPS, etc., and is due to the melting of preexisting low melting small and/or highly distorted. These crystals are produced during the annealing process, which increases size and perfection of those preexisting crystallites whose melting temperature lie below that of annealing temperature. As a result, the population that are recrystallized collectively in a small temperature range appears as an endothermic bulge in the DSC curves. This effect can readily be observed in Figure 3, where the DSC curves of fibers annealed at a series of annealing temperatures are shown for fiber spun at 3750 m/min. The position of this peak [Fig. 3(c)], as well as the crystallinity [Fig. 3(b)], increases with the annealing temperature.

The melting temperature remained almost the same up to a 220°C annealing temperature and slightly decreased at 240°C.

The Phase Behavior and Development of Orientation

Effect of Take-Up Speed on Crystallinity

We measured the crystallinity of these fibers by DSC and density gradient column techniques. As shown in Figure 4(a) and (b), the DSC data indicates the presence of 10% crystallinity at 500 m/min. The crystallinity from DSC was obtained by dividing the experimental heat of fusion data $\Delta H_{\text{exp.}} = (\Delta H_{\text{melting}} - \Delta H_{\text{cold crystallization}})$ with the heat of fusion of 100% crystalline PEN ($\Delta H°$

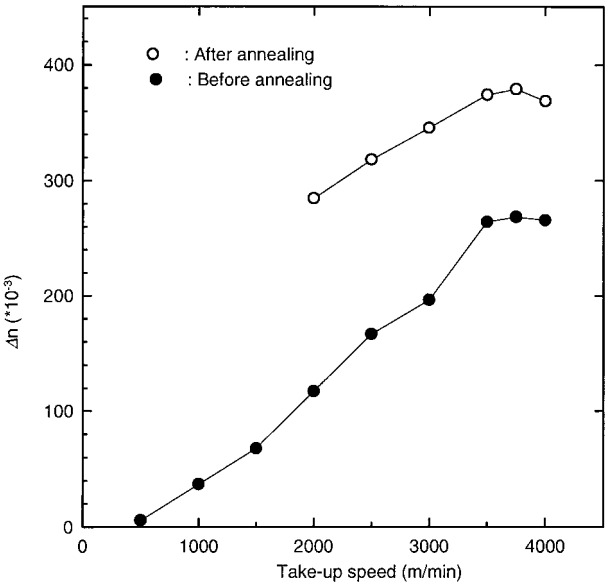

Figure 5 Birefringence of PEN fibers spun at different take-up speeds.

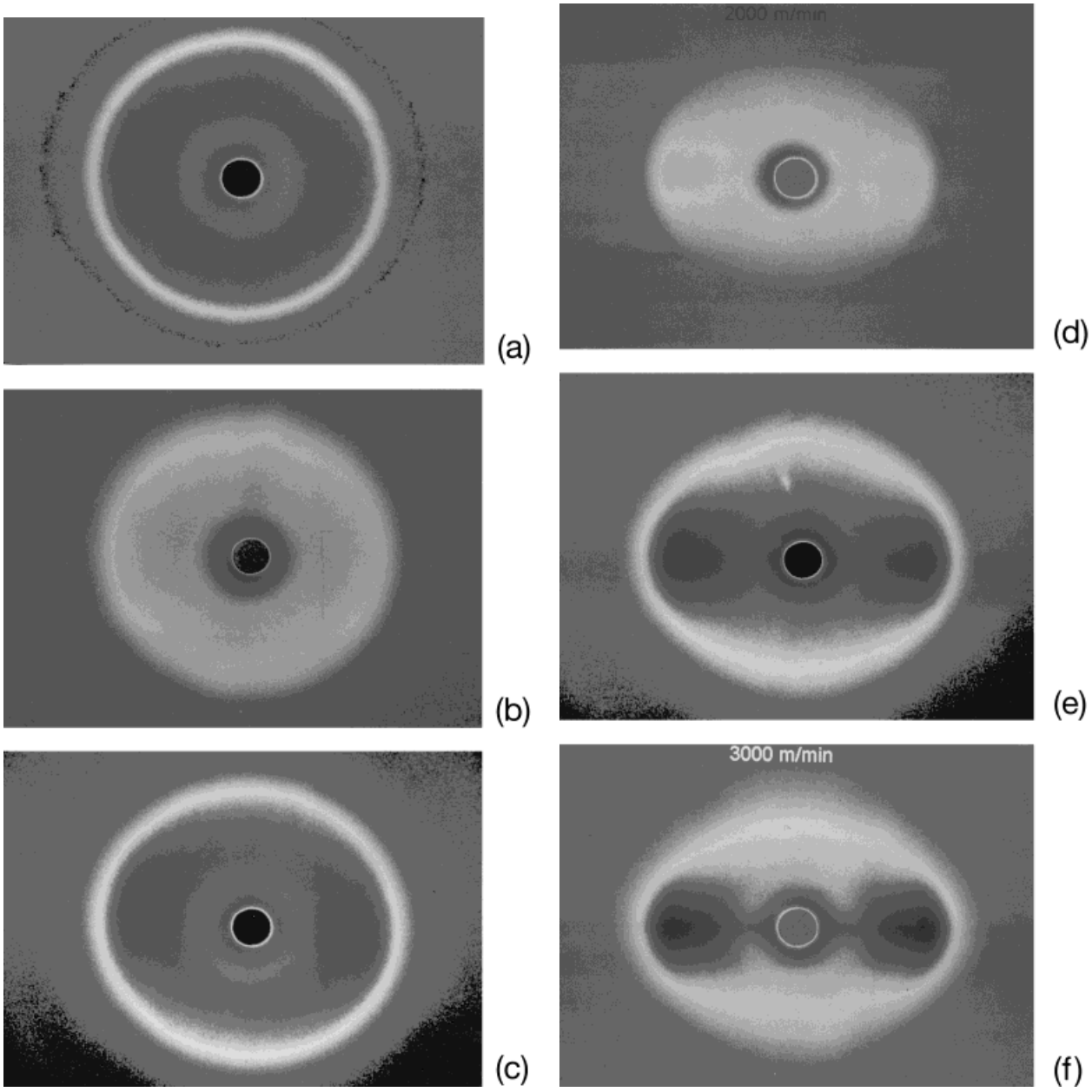

Figure 6 Wide-angle x-ray diffraction of PEN fibers. (a) 500 m/min; (b) 1000 m/min; (c) 1500 m/min; (d) 2000 m/min; (e) 2500 m/min; (f) 3000 m/min; (g) 3500 m/min; (h) 3750 m/min; (i) 4000 m/min.

= 103.7 J/g).[16] Crystallinity increases fairly linearly with the take-up speed up to about 3500 m/min and slightly decreases after this speed. The general trends in the density data are very similar to that obtained with DSC [Fig. 4(b)]. However, DSC gives higher crystallinities as compared to the density technique. This difference becomes as much as 20% in fibers spun at high speeds. This suggests that the literature value of ΔH° may be too low. The density technique, being nondestructive, may give accurate changes, particularly at low crystallinity levels in the absence of voids. The DSC technique sometimes results from the inaccurate determination of the baselines in the DSC curves. This also explains the density of the low speed spun fibers, which does not change significantly in the 500–1500 m/min range and then starts to increase. In DSC data this occurs around 1000 m/min.

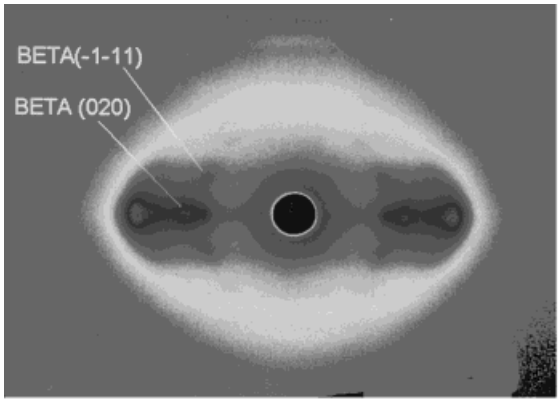

(g)

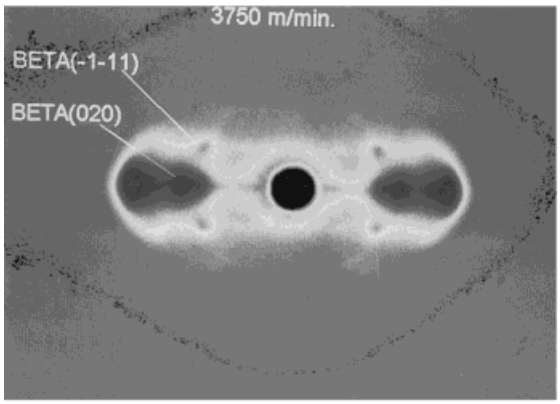

(h)

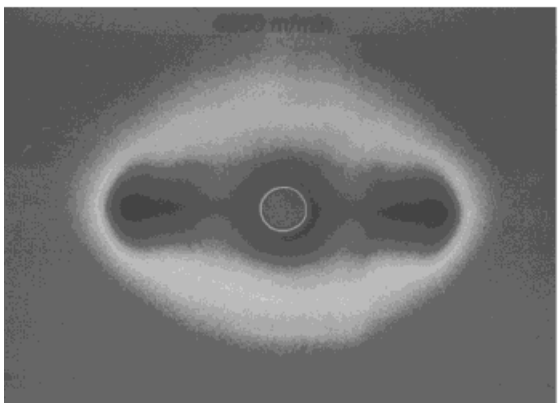

(i)

Figure 6 (*Continued from the previous page*)

Birefringence

The PEN fibers spun at 500 m/min showed almost "zero" birefringence (Fig. 5) (Δn_{12}, 1 = fiber axis, 2 = radial direction), indicating very low levels of orientation at this speed. Beyond 500 m/min it begins to increase fairly linearly with the increase of take-up speeds up to about 3500 m/min, then shows a slight decrease with further increase to 4000 m/min. Upon annealing, the birefringence increases by about 0.1, presumably as a result of increases in crystallinity during annealing. The birefringence of the fibers spun below 2000 m/min and annealed fibers could not be measured due to their opacity.

Wide-Angle X-Ray Diffraction

In order to investigate the development of crystallinity, orientation, and the phase behavior, we obtained WAXS film patterns on spun fibers. These are shown in Figure 6. The WAXS patterns taken on fibers with less than a 1500 m/min speed exhibit a fairly broad amorphous halo with little or no azimuthal intensity variations. At 2000 m/min, the concentrations of intensity in the equatorial direction is observed without the presence of discrete diffraction spots, indicating that while the orientation of the chains are occurring, they do not pack into a regularly repeating lattice structure. This does not occur until about 3500 m/min, at which speed discrete diffraction spots in the equator, as well as first layer lines are observed. The development of these patterns takes an unexpected turn beyond 3750 m/min, at which speed the discrete spots were observed to be the sharpest. At 4000 m/min, although the pattern is highly anisotropic, the discrete spots are greatly minimized, indicating that the crystalline order is significantly reduced at this speed.

As it can be seen more quantitatively in equatorial and meridional diffractometer scans of these unannealed fibers in Figures 7 and 8, the $\beta(020)$, together with the $\alpha(\bar{1}10)$ peak on the equator (Fig. 7), do not appear until the take-up speed reaches a critical value around 3500 m/min. The intensity of these peaks at the same location beyond 3750 m/min is greatly reduced. In the meridional scan only the a peaks are observed, and the broad amorphous halo spanning from 10 to 30° of 2θ reduces its intensity while the crystalline peaks belonging to the a form appear again above a critical value around 3500 m/min.

When these fibers were subjected to constrained annealing, the WAXS patterns showed increased preferential orientation along the fiber axis with the increase of the original spinning speed even in the 500–1500 m/min range, in which the precursor as-spun fibers did not show any preferential orientation [Fig. 9(a)–(c)]. The fibers spun at 500 m/min and 1000 m/min exhibit exclusively α-form, as indicated by the presence of peaks such as (010), (100), and $(\bar{1}10)$ at the equator. At and above a 1500 m/min spinning

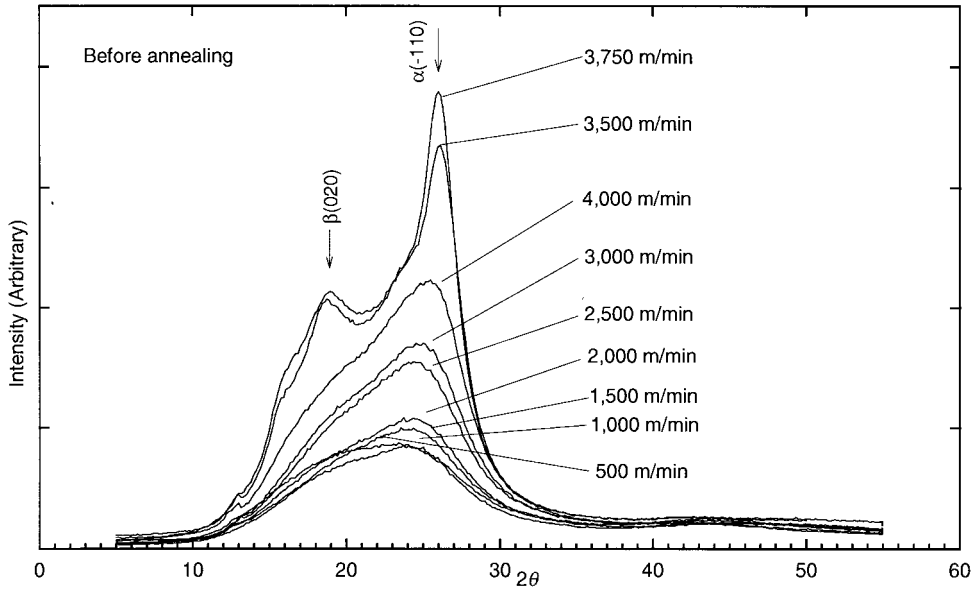

Figure 7 X-ray patterns of as-spun PEN fibers spun at different take-up speeds (Equatorial, Reflection).

speed, the heat set fibers begin to exhibit the α-form as well as the β-form. This is evidenced by the appearance of an equatorial β-form (020) peak as well as a β-form ($1\bar{1}1$) peak located at the first layer line. The equatorial diffractometer scans also show the development of this β-form (020) peak in Figure 10. The intensity of the diffraction planes belonging to the β-form remain relatively low at lower speeds and they do become sharper at take-up speeds in the range of 3500 to 3750 m/min, as is also evident on the equatorial diffractometer scans shown in Figure 10. They are then greatly reduced at 4000 m/min.

The identity of the crystalline peaks in the meridional diffractometer profile is indicated on each peak shown in Figure 11. At a 3750 m/min spinning speed, we observe an additional peak at 43°, which did not match any of the known a form peaks. It may be associated with the β-crystal form, whose detailed crystallographic analysis is currently lacking.

Crystallite Sizes

A peak separation technique using Pearson VII curves to fit the data profile was applied to WAXS 2 profiles to obtain details of structure development: namely, the crystallite sizes. Figures 12–15 show the peak separation result on the equatorial reflection scans taken from unannealed and annealed fibers. The crystal size, L, normal to the ($\bar{1}10$) planes (in a direction roughly normal to the naphthalene planes in the unit cell) are estimated from these separated peaks by using Scherrer's formula,

$$L = \frac{k\lambda}{\beta_{1/2}\cos(\theta)}$$

where

$K = \mathbf{1}$, $\lambda = 1.542$ Å,

$\beta_{1/2}$ = half width (radians),

θ = peak location.

Figure 15 shows the results. The crystal size of a ($\bar{1}10$) plane of modification in as-spun fibers increased as the take-up speed increased, but it suddenly decreased at 4000 m/min. Crystal sizes of the same plane in annealed fibers are much larger than those of as-spun fibers, as expected, and as a result of annealing, they attain about the same value, eliminating the differences that existed between the precursor fibers. Of course, in the derivation of Scherrer equation,[17] the broadening of the diffraction peaks as a result of disorder was not taken into account. Therefore, these data should be viewed with caution.

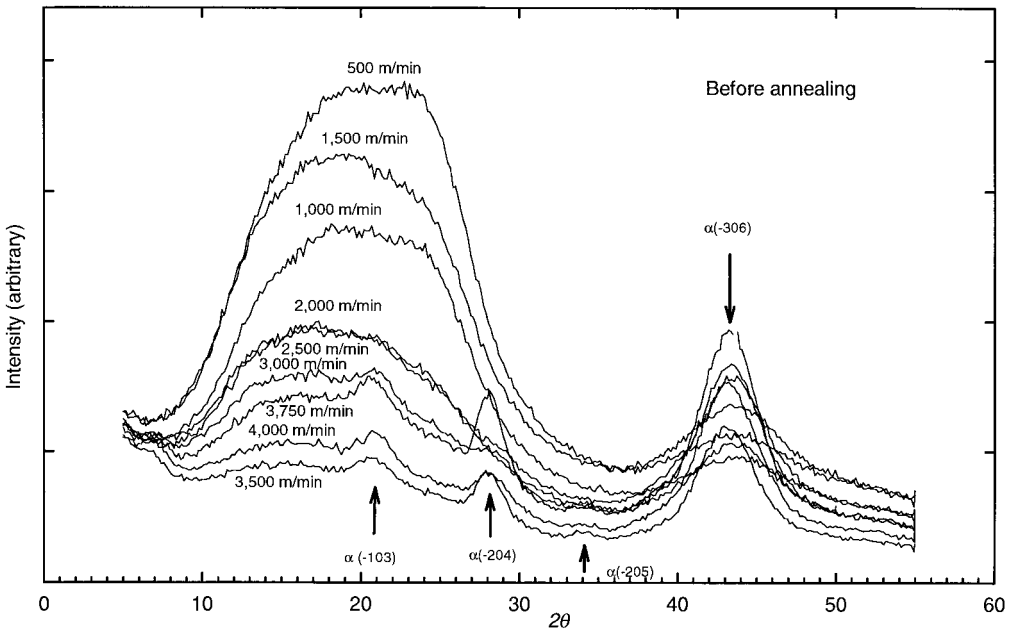

Figure 8 X-ray patterns of different take-up speed PEN fibers. As-spun fibers (Meridional, Transmission).

Orientation Behavior

In order to determine the preferential orientation behavior of the chain axes we used the pseudo-orthorhombic unit cell definition with Wilchinsky's rule.[18–21] With this definition of the pseudo-orthorhombic cell, it becomes easier to apply Wilchinsky's rule in order to determine the following orientation factors. Orientation factor of c-axis:

$$\overline{\cos^2\chi_{lc}} = 1 - 0.844 \times \overline{\cos^2\chi_1} - 1.156 \times \overline{\cos^2\chi_2}$$

where χ_1 = angle between the pole of $(\bar{1}10)$ and reference direction, χ_2 = angle between the pole of (010) and reference direction.

For this, the azimuthal intensity distributions of the $(\bar{1}10)$ and (010) planes were determined for annealed fibers, and using the equations given above, the f_c values were determined for the annealed fibers and are given in Figure 16. This also indicates a monotonous increase of c-axis orientation up to about 3750 m/min, beyond which a slight decline is observed.

SMALL ANGLE X-RAY SCATTERING

The as-spun fibers did not have sufficient scattering power due to the low crystallinities and poor electron density contrast between the phases. Therefore, the SAXS patterns were obtained only on the heat-set samples. As shown in Figure 17, the long period decreases with the increase of take-up speed up to about 2500 m/min and then shows a maximum around 3500 m/min before decreasing again. In addition, with the exception of 1000 m/min, the SAXS patterns exhibit a two 'line' intensity distribution whose width in the transverse direction increases indicating that the widths of the crystallites also decrease with the increase of take-up speed. It is also interesting to note that the upturn in the curve coincides with the appearance of discrete diffraction peaks in the WAXS patterns of the as-spun precursors. At 4000 m/min the scattering intensity is reduced while preserving the shape of the pattern possibly indicating partial destruction of superstructural order at this speed is also translated into their heat set counterparts.

Mechanical Properties

The stress strain curves for as-spun, as well as spun and annealed fibers, are shown in Figures 18 and 19, respectively. In as-spun fibers, the natural draw ratio, defined as a draw ratio at the point of strain hardening, decreased as spinning speed

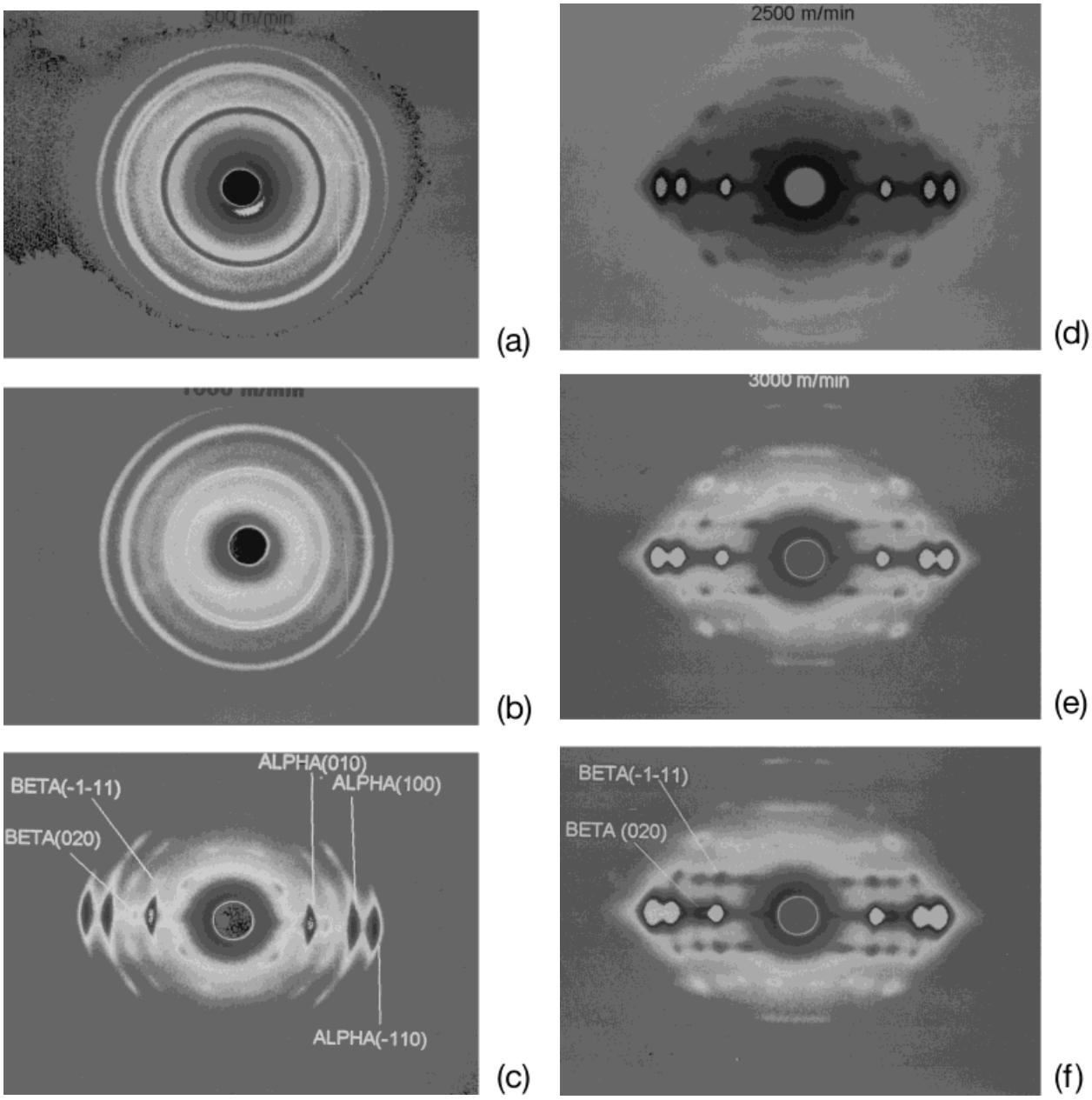

Figure 9 Wide-angle x-ray diffraction of annealed PEN fibers. (a) 500 m/min; (b) 1000 m/min; (c) 1500 m/min; (d) 2500 m/min; (e) 3000 m/min; (f) 3500 m/min; (g) 3750 m/min; (h) 4000 m/min.

increased and completely disappeared over 3000 m/min. These stress–strain curves show a yield point and stress drops after the yield, indicating development of neck or necks and a large plastic deformation section before the stress starts to rise again. The onset point at which the stress starts to rise, which may be called the natural draw ratio or the critical draw ratio at the onset of stress hardening, steadily decreases with the increase of take-up speed. The plastic deformation region essentially disappears above about 2000 m/min and, the stress–strain curves begin to resemble those of fully drawn fibers. As expected from the structural variations, the highest modulus and

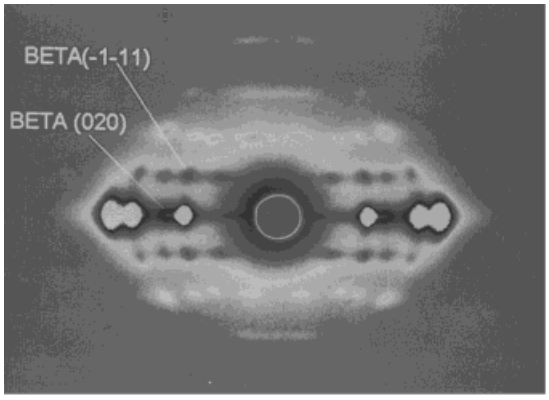

(g)

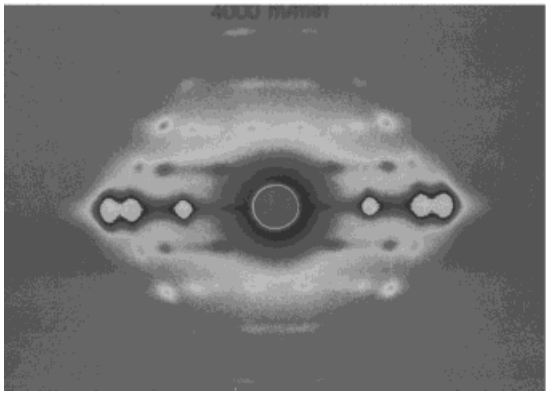

(h)

Figure 9 (*Continued from the previous page*)

tensile strength is observed in fibers spun at 3750 m/min. When the fibers are annealed, the stress–strain curves no longer show the stress drop after the yielding and elongation at break decreases rapidly. The Young's modulus, stress at break, and elongation at break, which change with take-up speed are shown in Figures 20–22 Modulus, as well as stress at break, increases as expected from the increases in crystallinity and chain orientation, while the elongation at break decreases. The fibers spun below 1500 m/min became too brittle to test upon their annealing at 220°. Even the fiber spun at 2000 m/min and subsequently annealed still showed large variations in their tensile properties. But above 2500 m/min, breaking stress and Young's modulus increased with take-up speed and showed maximum at 3750 m/min, like the fibers without heat treatment. As can be seen in Figures 21–22, stress and strain at break of annealed fibers were almost the same as those unannealed precursors, but modulus increased by about 15–20% presumably as a result of increased crystallinity.

Young's modulus is known to be related to molecular orientation in the fiber, and there are several reports that show a linear relationship between Young's modulus and birefringence of commercial fibers. Figures 23–24 show Young's modulus and stress at break as a function of birefringence. The stress at break increased linearly with birefringence; however, Young's modulus showed better linearity with density than with birefringence. This might indicate that modulus of PEN fiber is related more to the proportion of the crystalline regions in fibers than the level of their interconnectivity through their extended chains that pass through amorphous regions.

Stress at break and Young's modulus of annealed fibers showed good linearity with birefringence and density, as in the case of the unannealed fibers. However, the dependency on birefringence or density in annealed fibers, as determined by the slopes in figures, was much higher than that in unannealed fibers.

DISCUSSION

Orientation and Crystallization

At speeds up to 1500 m/min, the polymer chain axes increasingly orient in the fiber direction, as evidenced by the increase in birefringence. In this range, the density remains essentially constant and WAXS patterns show only an amorphous halo, clearly indicating the polymer chains orient but do not crystallize.

Figure 25 shows the relationship between density and birefringence of PEN fibers. It demonstrates a linear relationship with a slope change at $\Delta n = 0.09$. Similar results were reported also on high-speed spun PET fibers by Shimizu et al.[4] They explained this break point as a starting point for flow-induced crystallization. Wide angle x-ray patterns of PEN fibers showed a perfect amorphous halo up to 1500 m/min, which had $\Delta n = 0.07$, and this appears to support Shimizu et al.'s explanation. They also found that the position of this breaking point was a function of melt draw ratio and molecular weight. From the linear relationship between birefringence and density, intrinsic birefringence of 100% crystalline PEN $\Delta n^\circ = 0.791$ was extrapolated for the crystalline density of 1.407 g/cm^3. Constrained annealing increases the birefringence of the fibers without a loss of the linear relationship between density and

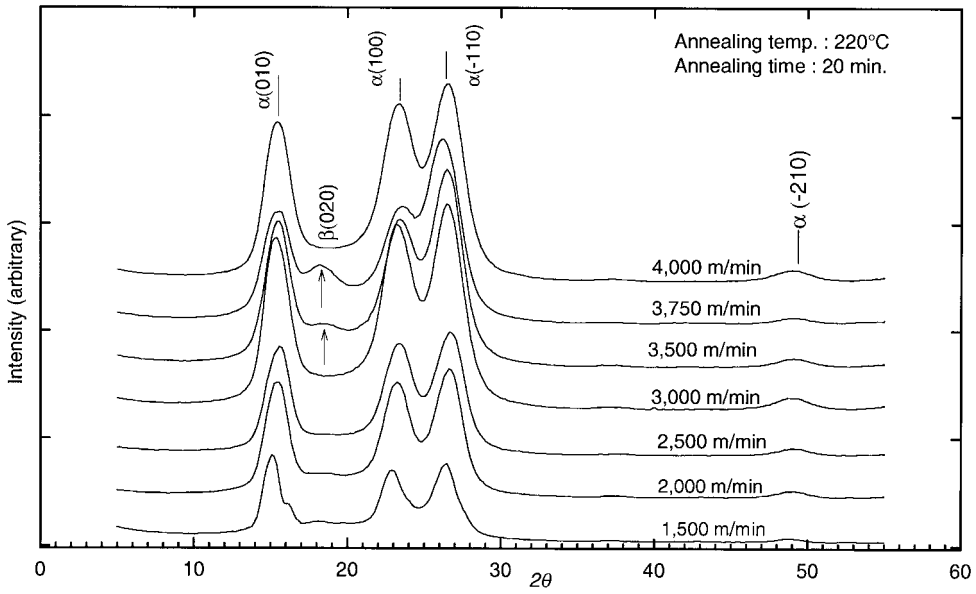

Figure 10 Wide-angle x-ray diffractometer scans of annealed PEN fibers (Equatorial, Transmission).

birefringence. One could also estimate the intrinsic birefringence of the amorphous regions assuming the proportionality constant k is the same for crystalline and amorphous regions in the following expressions

$$\Delta n_c^\circ = k \cdot \rho_c$$

$$\Delta n_a^\circ = k \cdot \rho_a$$

where Δn_c°, Δn_a°, ρ_c, ρ_a are crystalline and amor-

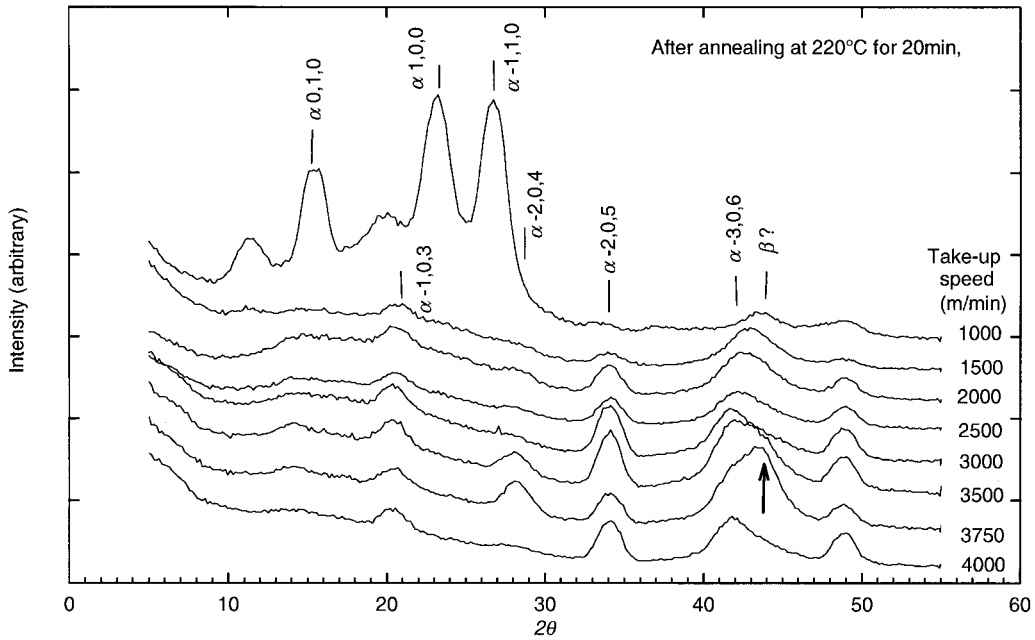

Figure 11 Wide-angle x-ray patterns of annealed PEN fibers (Meridional, Transmission).

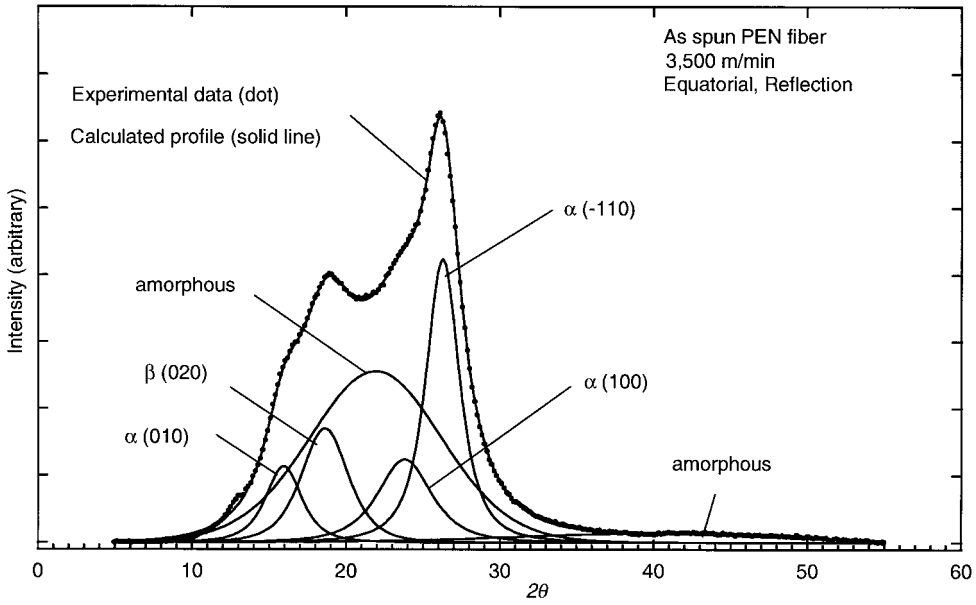

Figure 12 Peak separation of wide-angle x-ray profile of as-spun PEN fiber. Fiber was spun at 3500 m/min. Equatorial, reflection mode.

phous intrinsic birefringences and densities of 100% crystalline and fully amorphous PEN, respectively.

As discussed earlier, the birefringence of the as-spun fibers continue to increase, the WAXS patterns of the as-spun fibers do not show any crystalline diffraction peaks at speeds from 500 to 1500 m/min. This indicates that the polymer

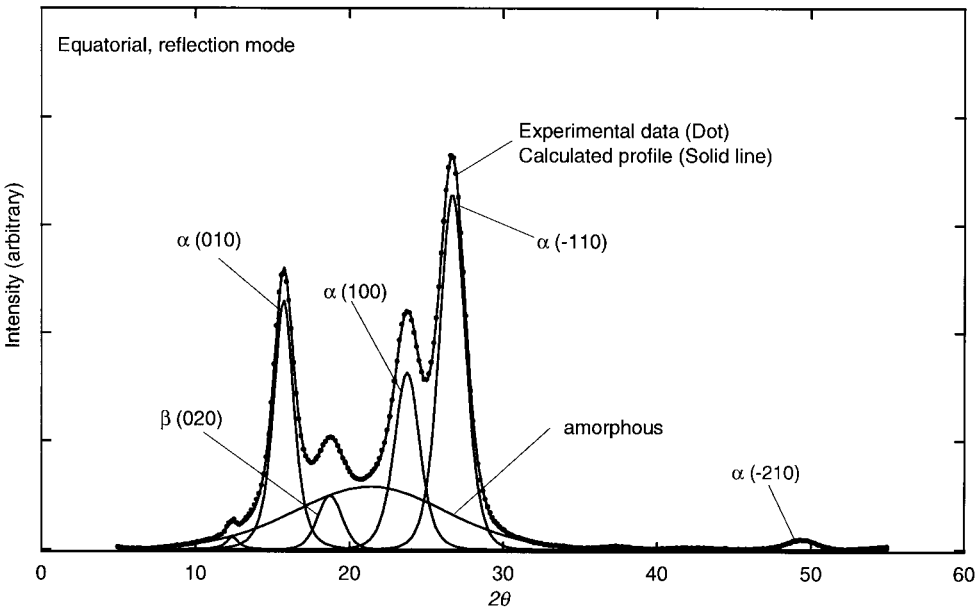

Figure 13 Peak separation of wide-angle x-ray profile of annealed PEN fiber. Fiber was spun at 3750 m/min and annealed at 220°C for 2 min.

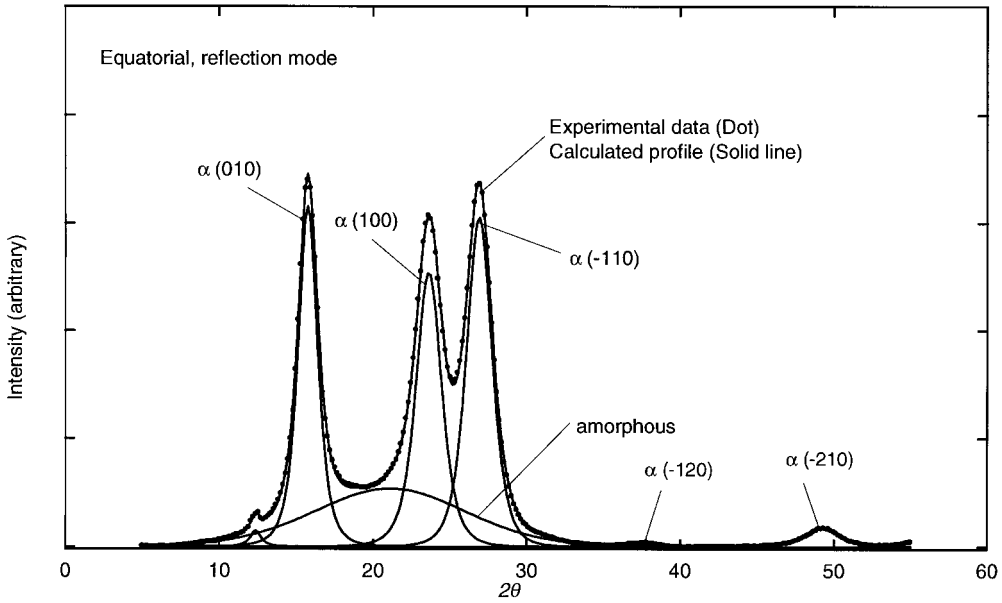

Figure 14 Peak separation of wide-angle x-ray profile of annealed PEN fiber. Fiber was spun at 4000 m/min and annealed at 220°C for 20 min.

chains oriented during spinning do not pack into regularly repeating crystalline lattice. Upon annealing, the fibers spun at 500 m/min increased in crystallinity without any sign of developing orientation in the crystalline regions. At 1000 m/min a slight preferential orientation accompanies the evolution of crystalline order. Substantial levels of orientation is observed at speeds 1500 m/min

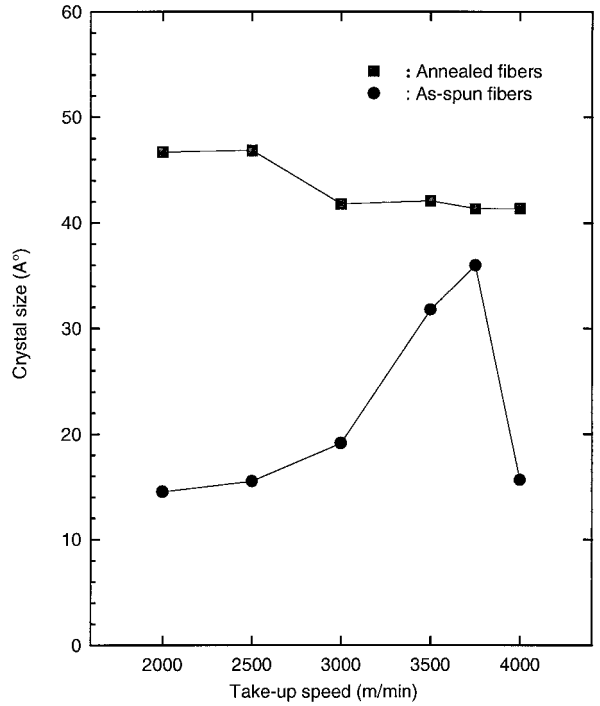

Figure 15 Crystal thickness change of a(−1,1,0) plant in as-spun PEN fibers.

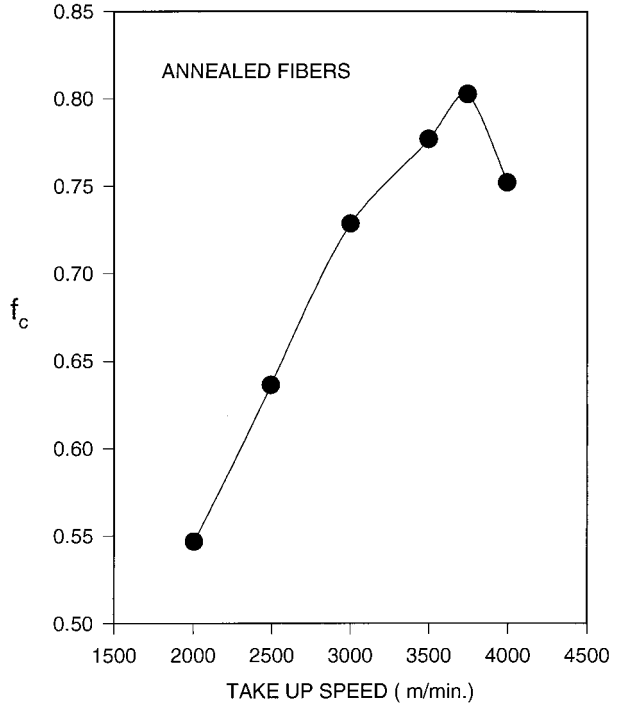

Figure 16 c-axis orientation factors for annealed PEN fibers.

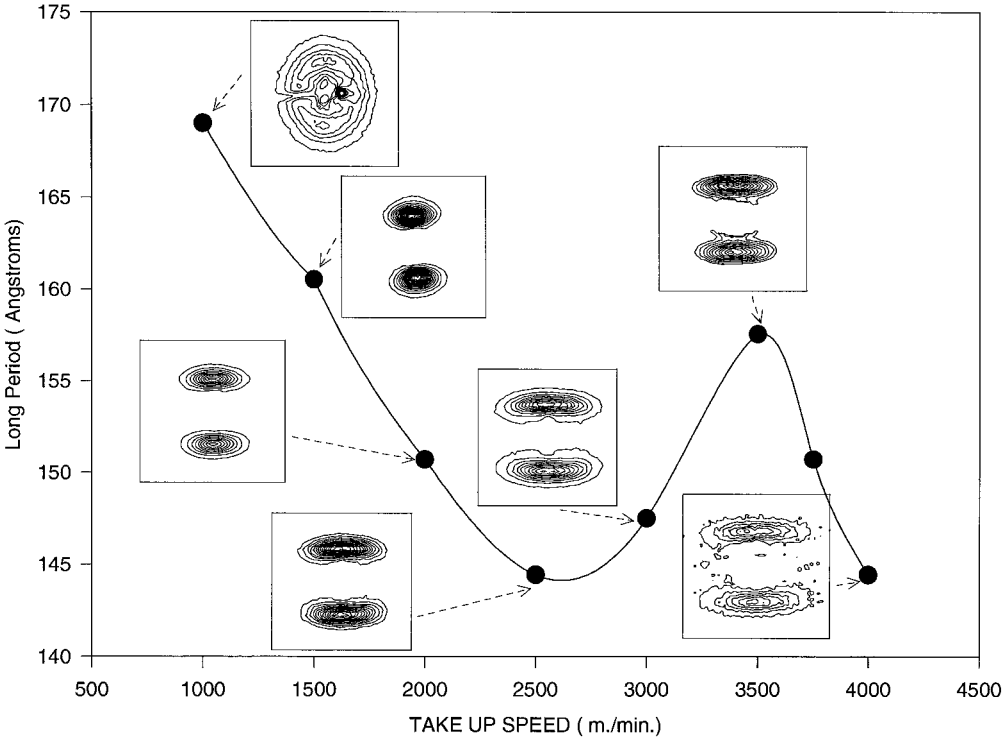

Figure 17 Long period vs. take-up speeds on PEN fibers melt spun and heat set at 200°C.

and above. This suggests that in order to develop orientation in the crystalline regions upon annealing, the as spun fibers should have a critical chain orientation, as measured by birefringence, between 0.04 (at 1000 m/min) and 0.07 (1500 m/min). Above this critical value, a portion of the

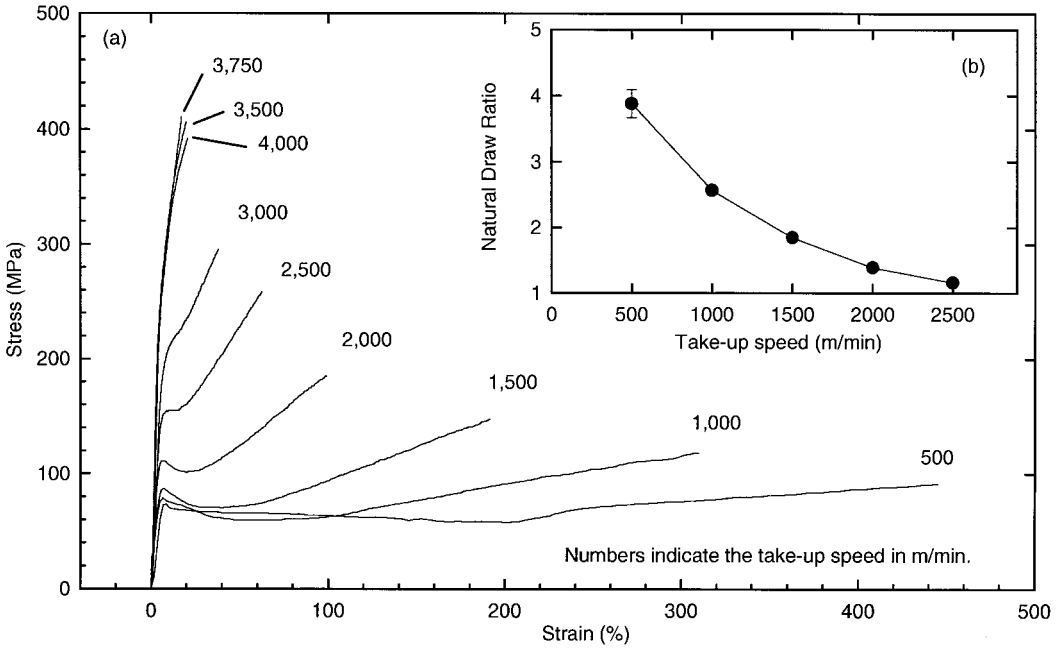

Figure 18 Stress–strain curves of PEN fibers spun at different take-up speeds.

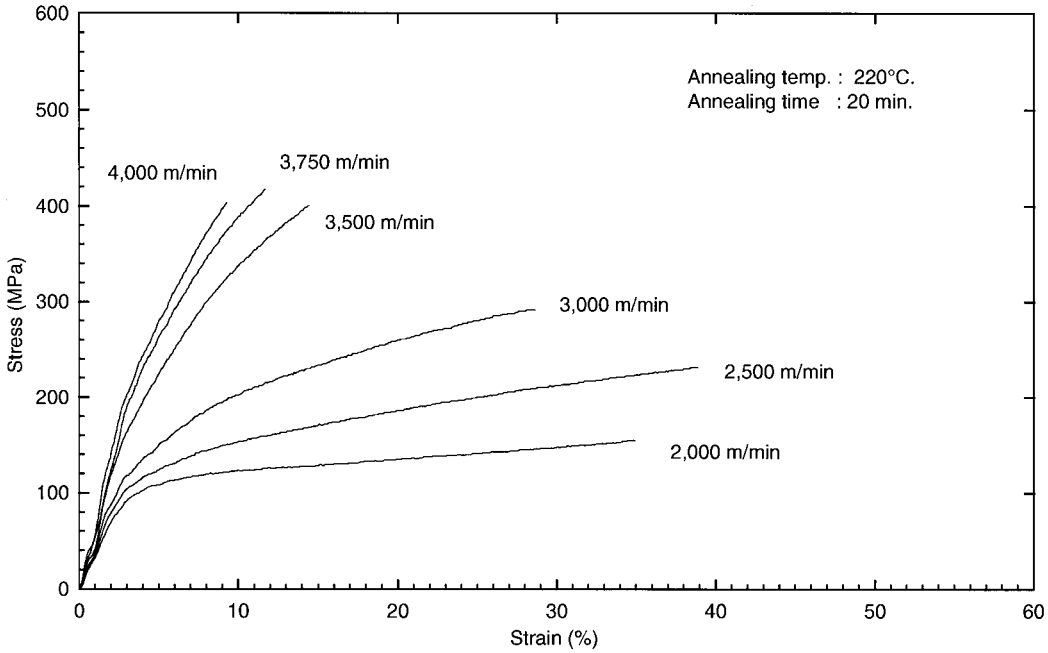

Figure 19 Stress–strain curves of annealed PEN fibers.

oriented chains pack into a crystalline lattice while a smaller portion remains in the amorphous state. Chain orientation below this critical value does not lead to the oriented crystalline regions, and upon annealing, however, the little orientation that was imposed during spinning relaxes, resulting in unoriented crystalline structure. Perhaps this critical value represents the minimum orientation levels at which sufficiently large crystalline nuclei form in the as-spun fibers, which in turn, are stable enough to grow at annealing temperatures.

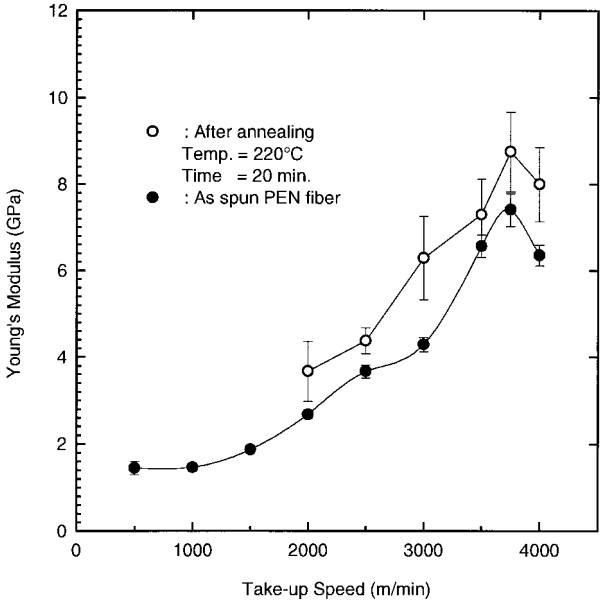

Figure 20 Change of Young's modulus by take-up speed.

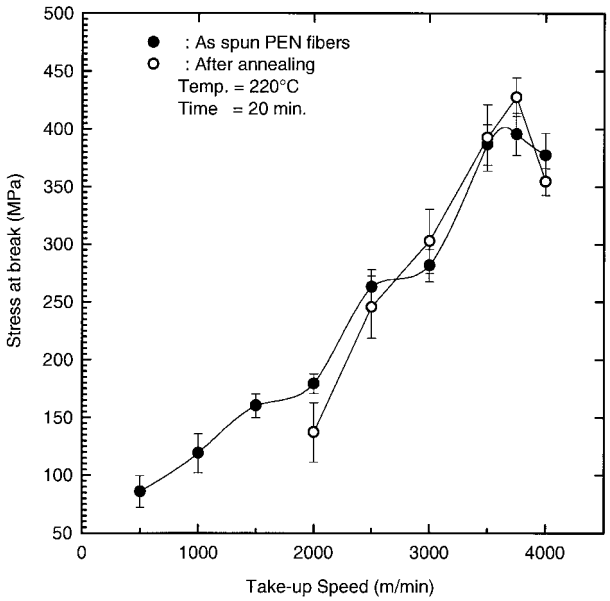

Figure 21 Breaking stress of PEN fibers of different take-up speeds.

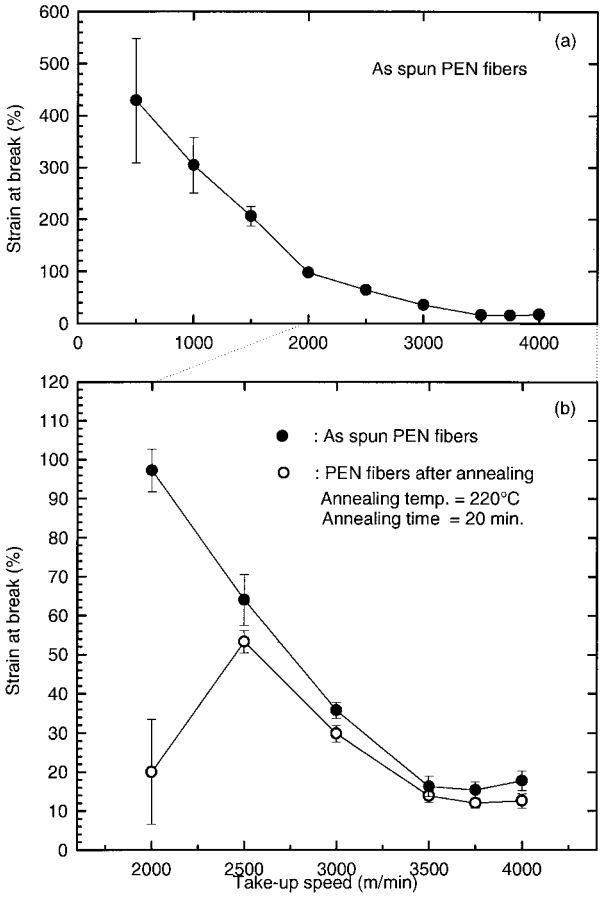

Figure 22 Strain at break of as-spun and annealed PEN fibers.

Crystalline Phase Behavior

PEN is known to have two crystalline forms, α and β. Our previous experimental work on quiescent state crystallization[22] showed that α-modification forms at temperatures below 220°C, and β-modification is observed at temperatures above 240°C. Both α and β forms were observed in PEN melt spun fibers and their relative proportion were found to depend on the take-up speed, as indicated by the x-ray data in Figure 7.

This take-up speed effect on crystal structure might be explained by the escalation of crystallization temperature caused by the increase in the take-up speed.[23] As the spinning speed increases, the temperature at which the crystallization occurs also increases as a result of increased stresses that individual chains experience during spinning. At low take-up speeds, the crystallization takes place at lower temperatures where the α modification is favored. As the spinning speed increases the crystallization temperature increases and the structure formation increasingly favors the formation of the β crystals.

At 4000 m/min, the WAXS pattern indicate highly oriented but disordered crystalline structure. Although we do not have direct evidence, this may have been caused by the appearance of neck-like deformation zone along the spinline. The existence of such regions results in fairly extensive localized deformation at relatively low temperatures. Under such processing conditions one normally obtains high orientation with distorted crystalline lattice as evidenced by the WAXS study. This certainly explains why the lattice structure is significantly destroyed, which resulted in the reduction in all other properties; crystallinity, tensile strength, modulus, etc. The fibers could not be spun beyond 4000 m/min under the conditions of the fibers spun in this research,

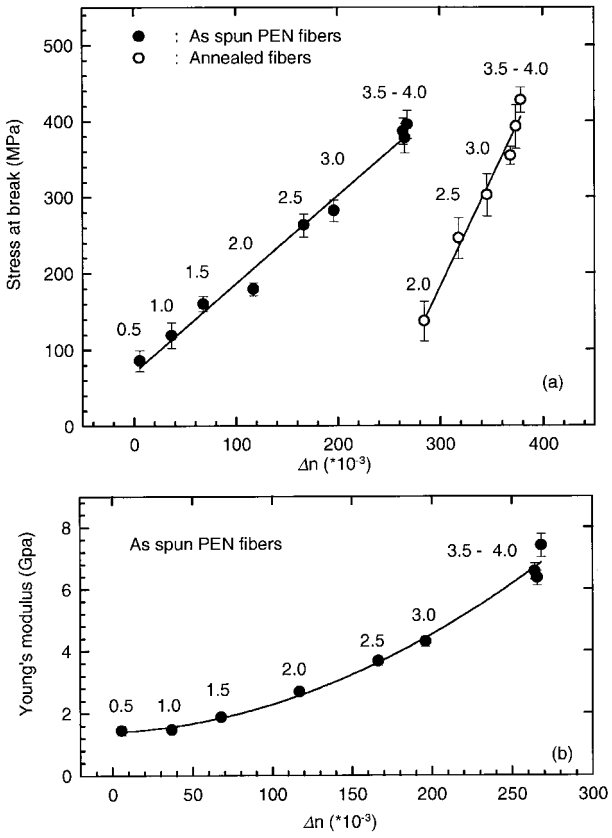

Figure 23 Stress at break and Young's modulus vs. birefringence. Numbers indicate take-up speed in km/min.

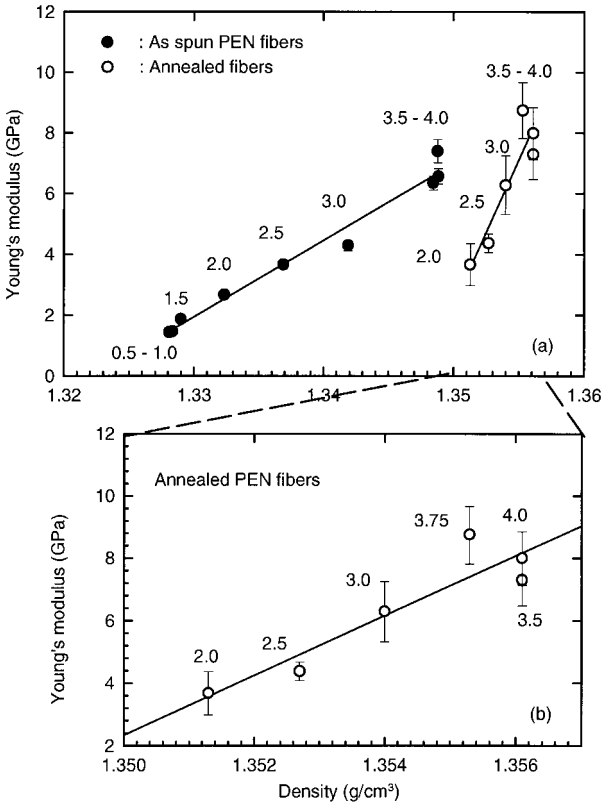

Figure 24 Density vs. Young's modulus of PEN fibers. Part b shows the detail of annealed fibers in part a. Numbers indicate take-up speed in km/min.

presumably as a result of increased levels of defects leading to catastrophic failure in the spinline.

CONCLUSIONS

The high-speed spinning studies we conducted revealed that PEN remains amorphous at low spinning speeds and crystalline order is established at speeds beyond 2500 m/min. The increase of take-up speed also increased the fraction of β phase in the crystalline regions, particularly beyond 3000 m/min. This α to β transition is as a result of increase in crystallization temperature with take-up speed. This also resulted in gradual increase of melting temperature as the β phase exhibit higher melting temperatures.

Annealing results in oriented crystalline fibers if the birefringence in the precursor fiber exceeds a critical value. This value was estimated to be in between 0.04 and 0.07. The spun fibers exhibiting birefringence less than this critical value do not form oriented crystalline domains upon constrained annealing. Our experimental results also indicate the intrinsic birefringence of 100% crystalline PEN is 0.791 and intrinsic birefringence value for the amorphous PEN is approximately 0.75.

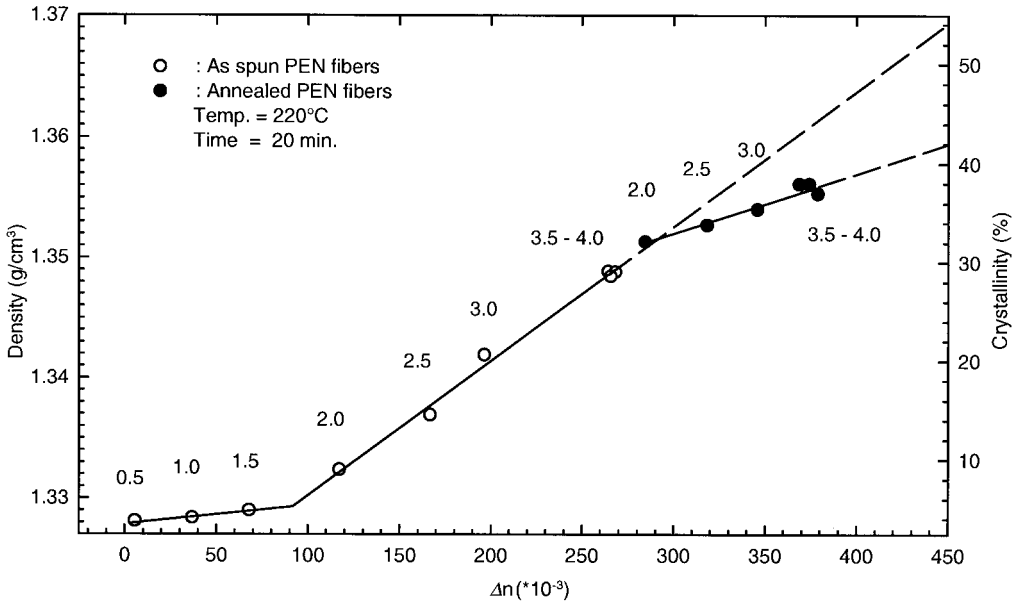

Figure 25 Bireringence vs. density of PEN fibers. Numbers indicate take-up speeds in km/min.

Parts of this work was presented at Beni-Bana Conference held in Zao, Japan (October 1994).

REFERENCES

1. H. M. Heuvel and R. Huisman, *High Speed Fiber Spinning,* A. Ziabicki, Ed., Wiley-Interscience, New York, 1985.
2. J. Shimizu, K. Toriumi, and K. Tamai, *Sen-i Gakkaishi,* **33,** T-208 (1977).
3. H. Yashuda, *High-Speed Spinning,* A. Ziabici and H. Kawai, Eds., John Wiley & Sons, New York, 1985.
4. J. Shimizu, N. Okui, and T. Kikutani, *High-Speed Spinning,* A. Ziabici and H. Kawai, Eds., John Wiley & Sons, New York, 1985.
5. M. Matsui, *High-Speed Spinning,* A. Ziabici and H. Kawai, Eds., John Wiley & Sons, New York, 1985.
6. Z. Mencik, *Chem. Prumysl.,* **17,** 78 (1967).
7. S. Buchner, D. Wiswe, and H. G. Zachmann, *Polymer,* **30,** 480 (1989).
8. I. Ouchi, H. Aoki, S. Shinotsuma, T. Asai, and M. Hosoi, Proc. 17th Japan Cong. Mater. Res, March 217 (1974).
9. S. Z. D. Cheng and B. Wunderlich, *Macromolecules,* **21,** 789 (1988).
10. S. Hayashi, M. Ishibarada, and S. Saito, *Polym. J.,* **17,** 953 (1985).
11. M. Cakmak, Y. Wang, and M. Shimhambhatla, *Polym. Eng. Sci.,* **30,** 721 (1990).
12. S. Murakami, Y. Nishikawa, M. Tsuji, A. Kawaguchi, S. Kohjiya, and M. Cakmak, *Polymer,* **36**(2), 2291 (1995).
13. M. Cakmak and S. W. Lee, *Polymer,* **36,** 4039 (1995).
14. J. C. Kim and M. Cakmak, *SPE Antec. Tech. Papers,* **41,** 1453 (1995).
15. Y. Ulcer and M. Cakmak, *Polymer,* **35,** 5651 (1994).
16. S. Z. D. Cheng and B. Wunderlich, *Macromolecules,* **21,** 789 (1988).
17. J. I. Langford and A. J. C. Wilson, *J. Appl. Cryst.,* **11,** 102–113 (1978).
18. Z. W. Wilchinsky, *J. Appl. Phys.,* **30,** 792 (1959).
19. Z. W. Wilchinsky, *J. Appl. Phys.,* **31,** 1969 (1960).
20. Z. W. Wilchinsky, *J. Appl. Polym. Sci.,* **7,** 923 (1963).
21. M. Cakmak and S. W. Lee, *Polymer,* to appear.
22. J. C. Kim and M. Cakmak, to appear.
23. H. Haberkom, K. Hahn, H. Breuer, H.-D. Dorrer, and P. Matthies, *J. Appl. Polym. Sci.,* **47,** 1551 (1993).